

Thrusting and sinistral wrenching in a pre-Eocene HP-LT Caribbean accretionary wedge (Samaná Peninsula, Dominican Republic)

Philippe Goncalves^a, Stéphane Guillot^{b*}, Jean-Marc Lardeaux^b, Christian Nicollet^a, Bernard Mercier de Lepinay^c

^a Laboratoire de géologie, université Blaise Pascal, CNRS - UMR 6524. 5, rue Kessler, 63038 Clermont-Ferrand cedex, France

^b Laboratoire de dynamique de la Lithosphère, UCB- Lyon et ENS-Lyon, CNRS – UMR 5570, 27, boulevard du 11 Novembre, 69622 Villeurbanne cedex, France

^c Geosciences Azur, CNRS-UMR 6526, 250 rue A. Einstein, 06560 Valbonne, France

Received 28 May 1999; accepted 15 November 1999

Abstract – The North Caribbean margin is an example of an oblique convergence zone where the currently exposed HP–LT rocks are systematically localised close to strike-slip faults. The petrological and structural study of eclogite and blueschist facies rocks of the peninsula of Samaná (Hispaniola, Dominican Republic) confirms the presence of two different metamorphic units. The former displays low metamorphic grade (Santa Barbara unit), characterized by the assemblage albite - lawsonite (7.5 ± 2 kbar and 320 ± 80 °C). The latter (Punta Balandra unit), thrust over the first unit towards the NW, and is characterized by the occurrence of blueschist and eclogite facies assemblages (13 ± 2 kbar and 450 ± 70 °C), within oceanic metasediments. The isothermal retrograde evolution occurred in epidote-blueschist facies conditions (9 ± 2 kbar and 440 ± 60 °C). The late greenschist facies evolution is contemporaneous with conjugate NW–SE extension and E–W strike-slip faulting. This late extension is for regional dome and basin structures. According to their lithotectonic, structural and metamorphic characteristics, the metamorphic nappe stack of Samaná may be interpreted as a fragment of an accretionary wedge thrust onto the North American continental shelf. Evolution of the wedge was associated with the active subduction of the North American plate, under the Greater Antilles arc, at the level of the Puerto Rico trench. During active Late Cretaceous convergence, the HP rocks were initially exhumed, within the accretionary prism, by thrusting parallel to the NE–SW direction of convergence. Subsequently, during the Eocene collision between the Caribbean plate and the North American margin, the installation of a transtensive regime of E–W direction supports the local development of conjugate extension of NW–SE direction that facilitated the final phase of exhumation of the HP rocks.

© 2000 Éditions scientifiques et médicales Elsevier SAS

subduction / exhumation / extension / strike-slip fault / North Caribbean margin / HP-LT metamorphism / accretionary wedge

Résumé – La marge nord-Caraïbe est un exemple de zone de convergence associée à des grands décrochements senestres, où les roches de haute pression-basse température sont systématiquement localisées près des grandes zones de décrochement. L'étude pétrologique et structurale des éclogites et des schistes bleus de la presqu'île de Samaná (Hispaniola, République Dominicaine) a permis de confirmer la présence de deux unités de degré métamorphique différent, défini par Joyce [13]. La première unité de bas degré (unité de Santa Barbara) est caractérisée par l'assemblage albite-lawsonite. Le pic du métamorphisme a été estimé à $7,5 \pm 2$ kbar et 320 ± 80 °C. La seconde unité (unité de Punta Balandra) chevauche la première vers le Nord-Ouest. Elle est caractérisée par la présence de boudins d'éclogite et de schistes bleus au sein de métasédiments océaniques. L'évolution métamorphique montre un pic du métamorphisme de l'ordre de 14 kbar–450 °C, suivie d'une rétro-morphose isotherme dans le faciès des Schistes Bleus à épidote (9 kbar–440 °C). L'évolution tardive dans le faciès schistes verts, est contemporaine d'une tectonique en extension, synchrone des décrochements senestres est-ouest. Cette extension est marquée au niveau régional, par une structuration en dômes et bassins associée à des failles normales conjuguées affectant la foliation principale D2. De part ses caractéristiques lithotectoniques, structurales et métamorphiques, le complexe métamorphique de Samaná correspond à un fragment du prisme d'accrétion océanique Crétacé supérieur charrié tardivement sur la marge continentale nord-américaine. Dans ce contexte de convergence, les roches de haute pression sont d'abord exhumées parallèlement à la direction de convergence NE–SW, en contexte de subduction active, à la faveur de chevauchements au sein du prisme. Puis, au cours de la collision

* Correspondence and reprints: sguillot@univ-lyon1.fr

Éocène, entre la plaque Caraïbe et la marge nord-américaine, la mise en place d'un régime global transtensif senestre de direction Est–Ouest favorise le développement local d'une extension conjuguée de direction NW–SE permettant la fin de l'exhumation des roches de haute pression. © 2000 Éditions scientifiques et médicales Elsevier SAS

subduction / exhumation / extension / décrochements / marge Nord-Caraïbes / métamorphisme de haute pression / basse température / prisme d'accrétion

1. Introduction

Exhumation processes of subduction-related high pressure (HP) are still a crucial problem despite thirty years of development of quantitative methods in tectonics and petrology [1–4]. The problem of exhumation has been generally approached in continental collision zones, where the pre-collisional evolution is often obliterated. In contrast, this early evolution history is well recorded in active subduction zones, often associated with strike-slip faults (e.g. Franciscan Complex in California [5]; New Caledonia [6] or the trench of Marianna [7]). Thus, the exhumation of HP rocks can completely or partly related to subduction processes [5, 8, 9], and is probably facilitated by active strike-slip faults [10, 11]. The examination of oblique subduction zones with exposed HP rocks is a useful approach to the broad question of exhumation processes. In order to do this, we examine the northern margin of the Caribbean plate characterized by active subduction, with wrench tectonics and exposed HP rocks. In this paper we present new structural and metamorphic data on the HP-LT rocks of the Samaná peninsula (Hispaniola, Dominican Republic) in order to reconstruct the possible mechanisms of exhumation of HP rocks occurring in an oblique subduction context.

2. Geological framework

The North Caribbean active margin is currently a zone of transpression related to the motion of the North American and Caribbean plates. This zone is characterized by a large sinistral strike-slip system with an east–west direction, relayed to the east by the south-vergent subduction of the North American plate under the Caribbean plate at the level of the Puerto Rico trench (*figure 1*). This margin is marked by a complex of volcanic arcs active from the beginning of the Cretaceous until the beginning of the Eocene and which have been dismembered by Tertiary sinistral strike-slip tectonics [12]. The island of Hispaniola is a fragment of this Cretaceous arc. In its northern part, fragments of the fore arc zone and the accretionary wedge outcrop, including the HP-LT rocks of the Samaná peninsula [13–15]. This metamorphic unit corresponds to a fragment of a broad complex of HP-LT metamorphism related to the subduction of the North American plate under the Greater Antilles. Eclogites

and blueschists have been recognized throughout this plate boundary, particularly in the Puerto Rico trench and in the Mona Canyon (close to the northern coast of Puerto Rico) [16, 17] but also in Cuba [18, 19, 20]. The peninsula of Samaná is limited to the north by the Puerto Rico trench and to the south by the sinistral Septentrional fault zone. It consists of a metamorphic complex unconformably covered by the Talanquera and of the Canita limestones, of Middle Miocene age [15, 21] (*figures 2 and 3*). The metamorphic complex is composed primarily of micaschists (Santa Barbara and Punta Balandra units) and of marbles (Majagual and Rincon units) (*figure 2*). Joyce [13] has defined three zones of different degrees of metamorphism. To the north, outcrops a zone of low temperature, characterized by the assemblage albite-lawsonite (Santa Barbara unit); to the south, outcrops a zone of HP rocks (Punta Balandra unit), where some blueschist and some eclogite facies rocks are intercalated within the micaschists, close to the Septentrional fault zone. Between them, an intermediate zone of 1 or 2 km width can be recognized, showing the assemblage epidote, relicts of glaucophane, actinolite, lawsonite, and albite. In the southern side of the peninsula, the sinistral Septentrional strike-slip fault is underlined by Pliocene conglomerates, made up of fragments of HP rocks and limestones [22]. The age of the sedimentary or volcanic protoliths of the metamorphic rocks is unknown. Sm/Nd dating around 80 Ma have been interpreted as eclogitization age [23, 24], whereas K/Ar dating around 40 Ma would correspond to the end of the exhumation [23].

3. Structural analysis

In the metamorphic units of Punta Balandra and of Santa Barbara (*figure 4*), several generations of structures have been recognized [13, and this work]. Tropical weathering does not allow us to construct a complete structural map of the studied zone. However, the coherence of our observations are evident on various north–south cross-sections and along the southern coast and allow us to propose a possible structural evolution for the Peninsula.

The first phase of deformation, recognized only in the Punta Balandra unit, corresponds to the transposition at the cm to m scale of relict bedding in the carbonates and in the schists into a schistosity S_1 . Locally, lenses of eclogite of centimetre to plurimeter in size are included in the S_1 foliation. The strong dispersion of the S_1 foliation planes by the subsequent deformation, D_2 and D_3 , does not allow complete restoration of S_1 to its initial orientation. The major deformation, D_2 , is observable everywhere in the studied sector. It is characterized by the development of recumbent folds of cm to m scale which deformed the S_1 foliation. The axes of the D_2 folds are oriented NW–SE and are often underlined by glaucophane. The axial plane of the D_2 folds is characterized by the preferred orientation of blueschist facies

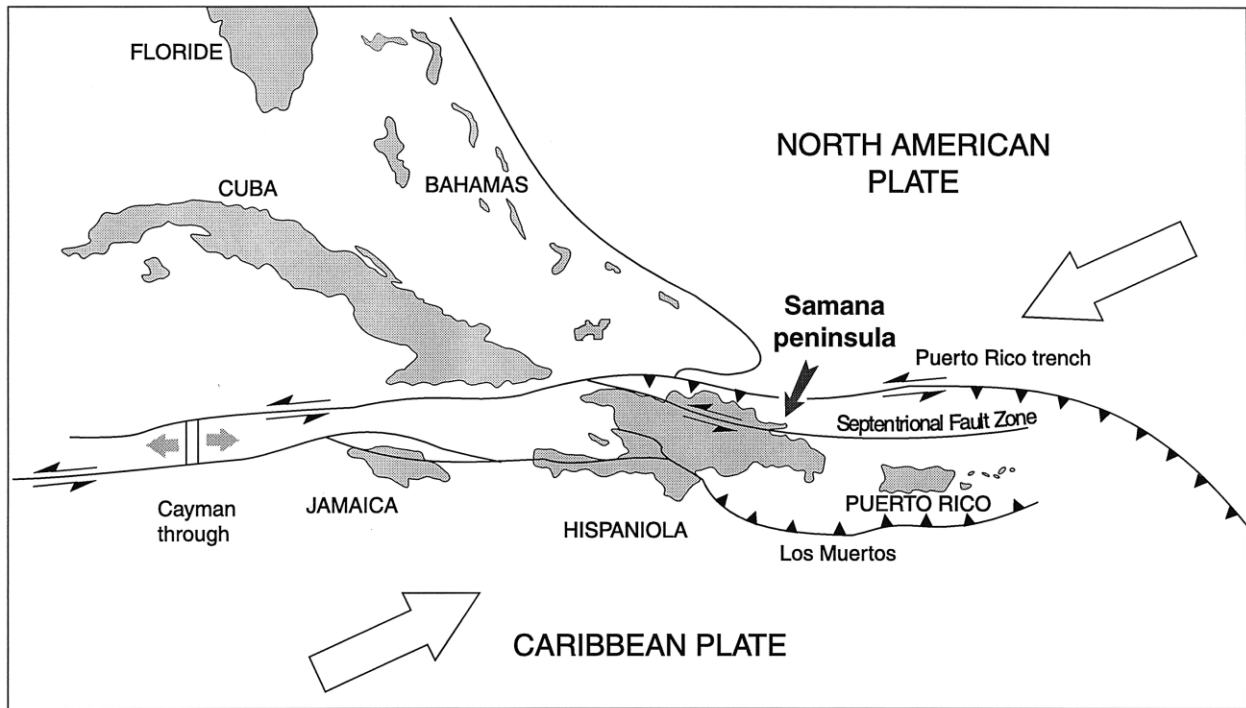


Figure 1. Location map and tectonic features of North Caribbean plate margin, modified from [14]. Arrows correspond to present-day direction of convergence.

Figure 1. Carte de localisation et structures principales de la marge Nord Caraïbes, modifié d'après [14]. Les flèches correspondent à la direction actuelle de convergence.

minerals (white micas, carbonates, glaucophane) defining the schistosity S_2 . Poles of the S_2 schistosity defer on a great circle whose axis orientation of $142N0^\circ$, is close to the axial direction measured for D_2 folds (figure 5). Locally, a $N15^\circ$ – $N35^\circ$ stretching lineation is observed on the S_2 plane, with a weak SSW plunging. The kinematic criteria associated with D_2 are scarce, however the asymmetry of the D_2 folds, systematically in Z and associated with a weak southward dipping of the S_2 schistosity, indicate a top-to-the-NE sense of thrusting. The obliquity of about 20 to 30° between the D_2 folds and the direction of stretching (figure 5) suggests a component of sinistral wrenching during D_2 .

A third generation of structures (D_3), is characterized by the occurrence of late NNE microfolds developed under greenschist facies conditions [13]. Associated with these microfolds, we have observed normal ductile shear planes, always conjugate with ENE–WSW strike and dip of about 30° towards the NNW and the SSE (plate 1: photo A). The shear planes bear as mineral lineation actinolite and chlorite with WNW trend (figures 4 and 5). These observations allow us to put forward the existence of a syn-convergence extension of NW–SE direction. The interference between the NW–SE D_2 folds and the ENE–WSW C_3 shear planes is responsible for the development of dome and basin struc-

tures at the metre to hectometre scale (figure 3). As for the D_2 phase, the obliquity between the dip of the C_3 planes and the direction of the L_3 lineation (figure 5) suggests a sinistral component during D_3 . The limestones of the Talanquera, which rest in discordance on the metamorphic units, were not affected by this phase of extension, suggesting a pre-Miocene age for the extensional tectonics.

The last generation of structures is contemporaneous with the sinistral motion along the Septentrional fault zone since the Pliocene [14, 22] transposed locally the different generations of structures.

4. Petrological analysis and mineral chemistry

In the Punta Balandra unit, we studied the eclogitic lenses S223 and SA34 in detail and their many-dm-size rims of retrograde metamorphism in the blueschist facies (sample SA33) and the glaucophane bearing micaschists SA28 and SA13. All these samples are located near the Septentrional fault, east of Samaná. The basic rocks probably derived from oceanic tholeiitic basalts [13]. From the Santa Barbara unit, only one well-preserved sample is studied (micaschist SA2).

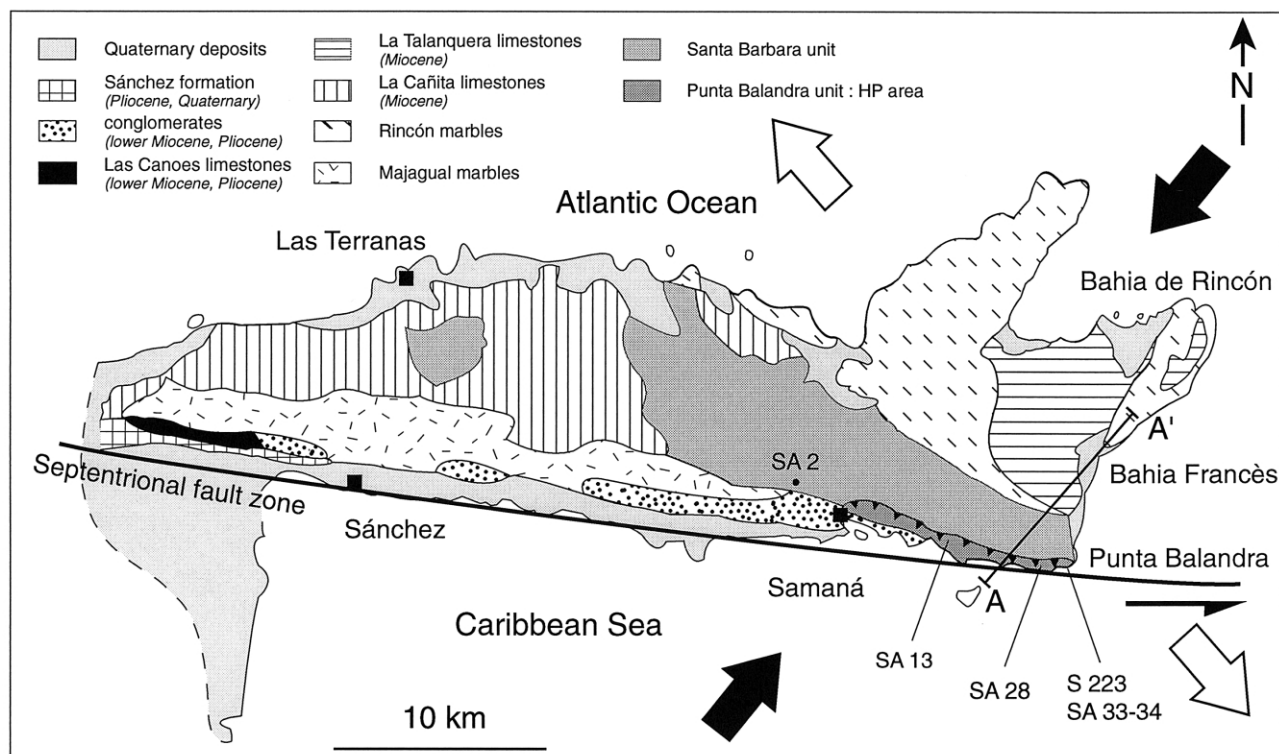


Figure 2. Geological map of Samaná peninsula, Hispaniola [13, 14]. SA2, SA28, SA33-34, S223 = investigated samples. NW–SE extension (white arrows) is perpendicular to pre-Eocene direction of convergence (black arrows). See text for further discussion. A–A': location of figure 3.

Figure 2. Carte géologique de la Péninsule de Samaná, Hispaniola [13, 14]. SA2, SA28, SA33-34, S223 = échantillons étudiés. Noter que la direction d'extension NW–SE (flèches blanches) est perpendiculaire à la direction ante-Eocène de convergence (flèches noires). A–A' : localisation de la figure 3.

The minerals were analyzed on a CAMECA SX 100 microprobe at the laboratory of geology of the University Blaise Pascal (Clermont-Ferrand). The analytical conditions were of 15 kV, 10 nA for a counting time of 10 s. Natural minerals were used as standards. Representative analyses are reported in table 1.

4.1. The Santa Barbara unit

The micaschist SA2 contains some nodules of albite, lawsonite, white micas, titanite and rare small garnets (size lower than 0.25 mm) in a matrix of quartz and calcite (plate 1: photo B). Lawsonite forms small well crystallized mineral of size lower than 0.2 mm in inclusions in albite nodules or in the matrix. Its Fe_2O_3 content is weak (< 1.1%), and the compositions are very close to the end-member $\text{CaAl}_2\text{SiO}_7(\text{OH})_2\text{H}_2\text{O}$. A foliation synchronous to the albite-lawsonite-garnet paragenesis is marked by the preferred orientation of white micas and by the concentration of oxides in these levels, corresponding to a deformation by dissolution-recrystallization. In this foliation, kink bands in

calcite indicate the low temperature conditions of the deformation. Garnet is composed of $\text{Alm}_{21-33}\text{Gross}_{25-29}\text{Pyr}_{2-3}\text{Spess}_{39-49}$. The Si^{4+} of phengites varies from 3.37 to 3.39 pfu. Lawsonite has a low Fe_2O_3 content (< 1.1 wt.%), and the compositions are very close to the end-member $\text{CaAl}_2\text{SiO}_7(\text{OH})_2\text{H}_2\text{O}$. The submillimetric nodules of plagioclase correspond to pure albite $\text{Ca} < 0.1$ wt.% and $\text{K} < 0.1$ wt.%).

4.2. Unit of Punta Balandra

This unit also consists of micaschists, locally very altered, and containing well preserved centimetre to metre lenses of basic rocks. The metabasalt S223 is massive, it is composed of euhedral garnet (up to 3 mm in size), clinopyroxene, glaucophane, phengite, zoisite, rutile, actinolite and quartz. Zoisites are particularly abundant in mono-mineralogic levels (plate 1, photo C). Omphacite is rare and appears in the form of small colourless rods of millimetre-length sizes in the matrix and at the rim of garnets. The two amphiboles present automorphic basal sections of very small size, without any

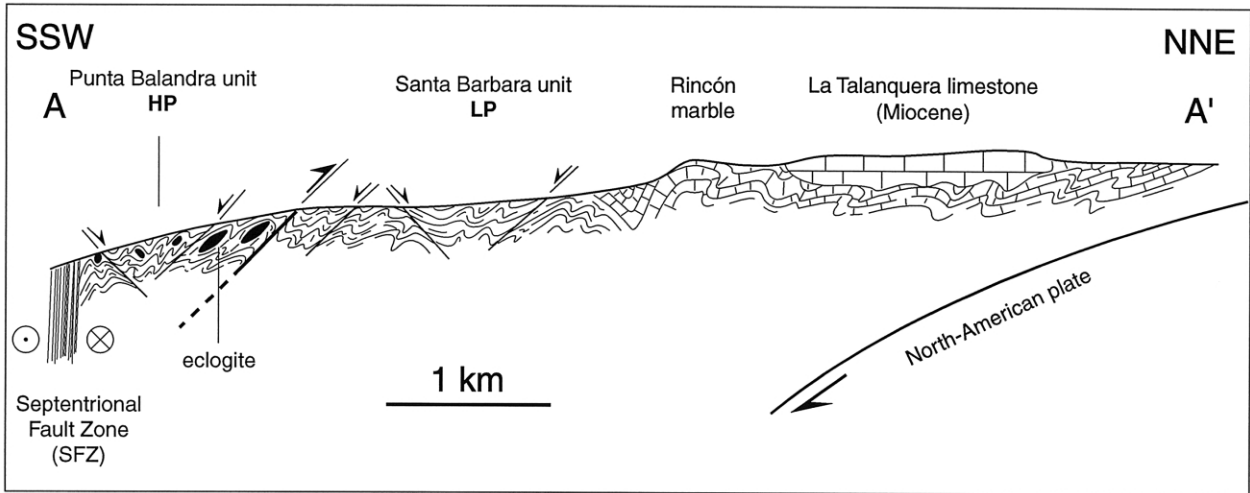


Figure 3. Cross-section A–A' of metamorphic units and limestones of the Samaná peninsula.

Figure 3. Coupe A–A' dans les unités métamorphiques et les calcaires de la péninsule de Samaná.

sign of destabilisation. It would seem, according to the petrographic observations, that glaucophane is post-eclogite facies paragenesis. The metabasalt SA34 is composed of a finely crystallized matrix containing mainly garnet porphyroclasts and broad pale green crystals of clinopyroxene, of millimetre size. Clinozoisite always intimately associated with paragonite forms clusters within the matrix. The late greenschist facies evolution is marked by the occurrence of carbonate, albite and chlorite, within the matrix and in the fractures of garnet.

Sample SA33 corresponds to the retrogressed rim of the eclogitic boudin SA34, including relicts of garnet and clinopyroxene. This latter is strongly retrogressed into finely crystallized glaucophane (*plate 1: photo D*). The mineralogy of the rock is composed of glaucophane, actinolite and oriented phengite underlying the blueschist foliation. The association of sodic and calcic amphiboles (SA33) is usual in eclogite and blueschist facies assemblages [25]. However, the absence of glaucophane in fresh eclogite SA34 clearly states that glaucophane present in the associated SA33 blue-

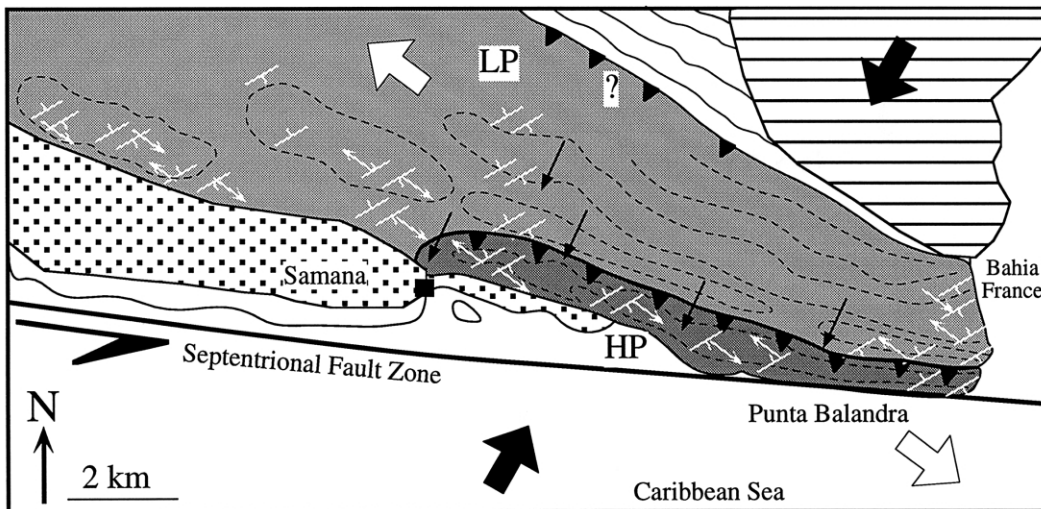


Figure 4. Structural map of Samaná peninsula; dotted lines = S_2 foliation trajectories, white symbols = D_3 structures.

Figure 4. Carte structurale de la péninsule de Samaná, les lignes pointillées représentent les trajectoires de foliation S_2 ; les symboles blancs représentent les directions structurales D_3 .

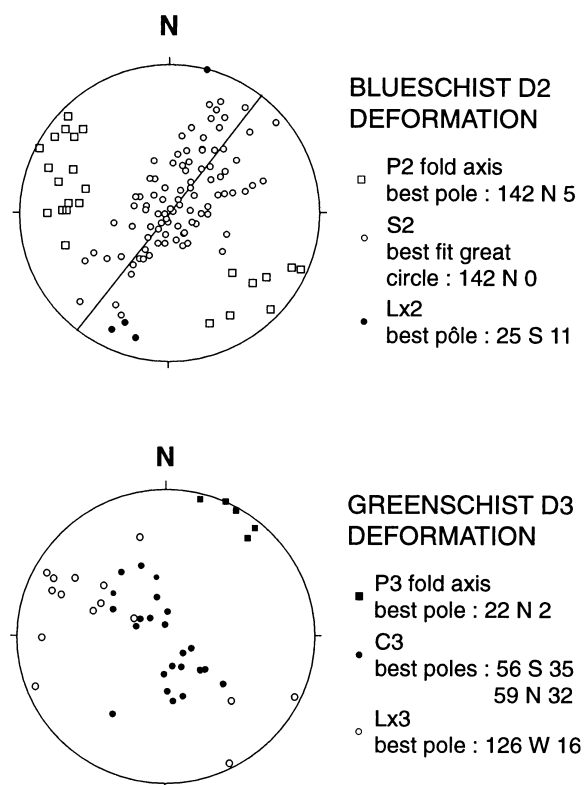


Figure 5. Lower hemisphere equal area projection of structural data: A) blueschist facies D_2 deformation; B) greenschist facies D_3 deformation.

Figure 5. Projection en hémisphère inférieure des données structurales : A) Schistes bleus D_2 ; B) Schistes Verts D_3 .

schist facies sample is a post-eclogitic phase as observed in the sample S223. The core of SA33 garnet contains zoisite and small crystals of titanite underlying a first foliation. Garnet rims contain actinolites, clinopyroxenes and phengites. The sigmoidal shape of the rim suggest synchronous crystallization of garnet and various inclusions under blueschist conditions. The final stage of the metamorphic evolution corresponds to the assemblage albite-chlorite-carbonate, locally crystallized in the fractures of garnets and in the matrix.

Micaschists SA28 and SA13 are composed of a matrix of quartz and calcite associated with large dark blue glaucophane crystals, which can reach 0.5 cm in length, epidotes (clinozoisite in inclusions in glaucophane, zoisite in the matrix), and white micas (paragonite in inclusion in glaucophane and phengite in the matrix). The preferred orientation of glaucophanes and phengites underlines the D_2 foliation. Largely altered garnets, in the sample SA13, contain inclusions of lawsonite (plate 1: photo D). Deformation D_3 causes the systematic stretching of the glaucophanes perpendicular to their long axis and the necks are filled by cal-

cite (plate 1: photo F). Some glaucophanes are affected by extensive C'-S structures, underlined by chlorite and secondary white micas, typical of the deformation D_3 (plate 1: photo E).

In the metabasalts (S223, SA33 and SA34) of the HP unit, the composition of garnets varies from $Alm_{48}Gross_{26}Pyr_4Spess_{0.5}$ to $Alm_{61}Gross_{43}Pyr_{20}Spess_8$. They are typical garnets of eclogites of the group C [26] and show a good homogeneity between the various samples (figure 6). Zoning in garnet S223 is characterized by a large core with a relatively constant composition and a thin rim with MgO increase FeO decrease. The CaO content is constant (figure 7). The observed evolution towards the rim is typical of a temperature increase at the end of garnet crystallization. Garnets of eclogite SA34 and blueschist SA33 show the same compositional variations consisting of an increase of FeO and MgO and a decrease in CaO and MnO from core to rim (figure 7). The FeO and MgO evolution is in fact related to an increase in the $Mg/(Mg + Fe^{2+})$ ratio, classically associated with a prograde crystallization [27]. Garnets of the micaschist SA13 is a solid solution of $Alm_{49-54}Gross_{27-31}Pyr_{4-5}Spess_{15-18}$. Their pervasive alteration did not make it possible to highlight a zonation.

Pyroxenes are only present in the basic rocks of the HP unit (S223, SA33 and SA34). According to the IMA classification [28], they fall into the field of omphacites (figure 8). In the eclogite S223, their jadeite content varies from 36 to 45 %. Clinopyroxene of eclogite SA34 is very abundant and is presented in the form of broad pale green crystals, their jadeite content varies from 42 to 49 %. In the metabasalt SA33, rare omphacites appear as relicts in the matrix, generally preserved in the pressure-shadows of garnets, or as inclusions within the garnet rim. These relict pyroxenes have a jadeite content ranging between 38 and 41 %. The difference in pyroxene composition between samples SA33 and SA34 is related to a reduction in Al and Na content probably due to the partial reequilibration of the clinopyroxenes under the blueschist facies conditions.

Amphibole only present in the HP unit of Punta Balandra is primarily in the form of glaucophane sometimes associated with rare actinolites. The low Fe content ($Fe_{tot} = 7.3$ to 9.4 wt.%) confers a pale blue colour to the glaucophane. In the micaschists SA28, the FeO content of glaucophane is higher than 11 wt.%, which explains its dark colour.

The three recognized populations of phengites according to their order of crystallization (included in garnets, in the S_2 foliation or associated with calcite, epidote and chlorite) show a slight decrease of Si^{4+} content from 3.47 to 3.27 pfu. Paragonite is present as inclusions in amphiboles of the SA28 ($NaO = 6.8$ wt.%) and SA34 eclogite, where it is closely associated with clinozoisite ($Na_2O = 6.5$ to 7.8 wt.%). The chemical composition approaches the paragonite end-member ($Pa_{88}Mu_{12}$ to $Pa_{98}Mu_2$, for eclogite SA34).

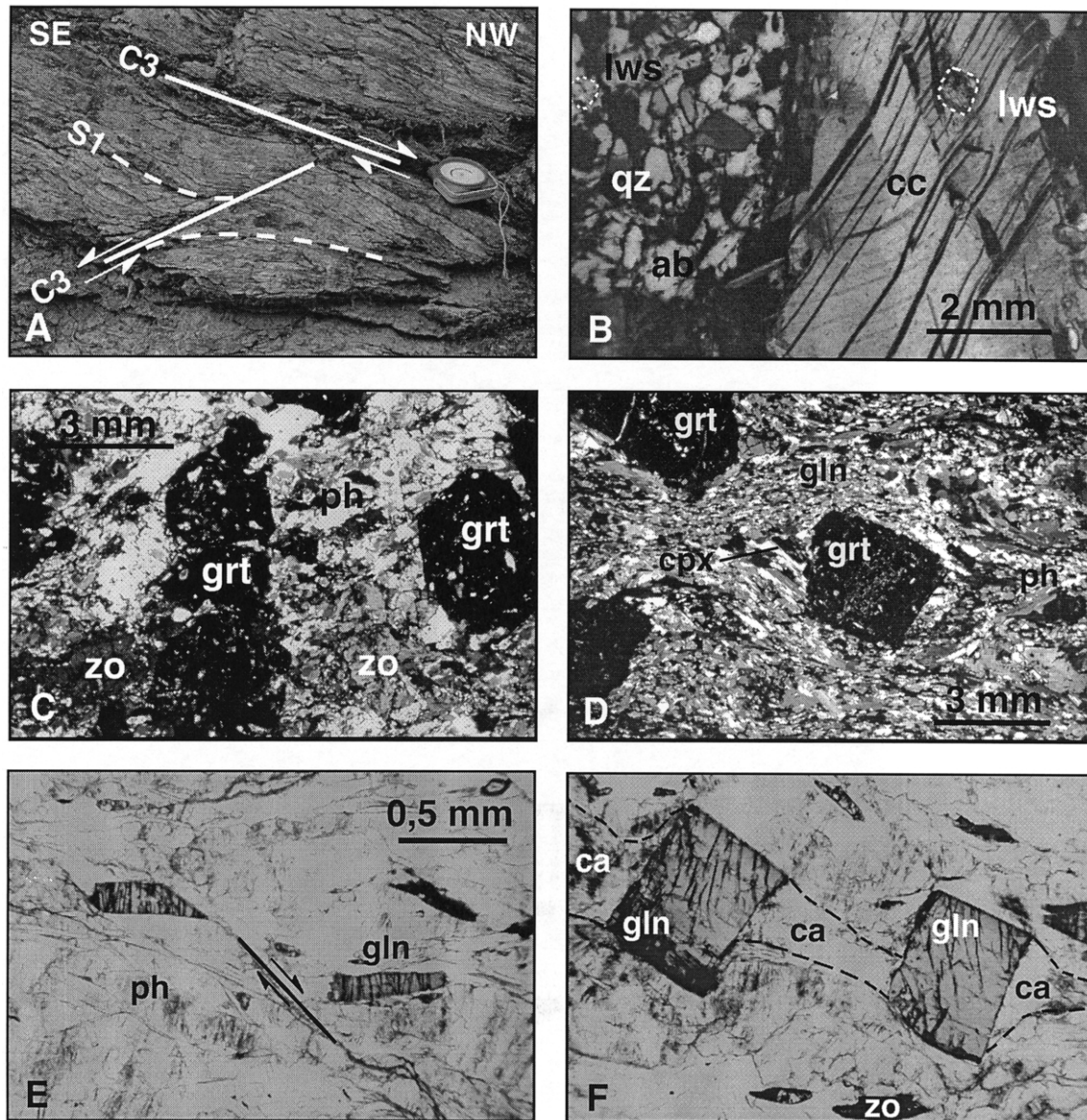


Plate 1. Photo A: Extensional tectonic within calcschists of Santa Barbara unit. The S_1 foliation (dotted line) is deformed by conjugate normal shear plane (C_3), sample SA 2. Photo B: Albite-lawsonite calcschist with albite nodule with inclusions of quartz and lawsonite. The calcite twins record a very low temperature deformation, Sample SA 2. Photo C: Low-T eclogite with garnet porphyroblast and zoisite, sample S223. Photo D: Blueschist. Garnet porphyroblasts with inclusions of zoisite and titanite surrounded by a blueschist foliation defined by glaucophane and phengite; clinopyroxene, partly preserved in garnet shadow, is transformed to glaucophane, sample SA33. Photo E: Glaucophane-bearing calcschists with extensional shear zone C_3 over S_2 foliation defined by phengite and glaucophane, sample SA28. Photo F: Glaucophane-bearing calcschists, extensional tectonics are indicated by microboudinage perpendicular to the long axis of glaucophane, necks of boudins are filled by calcite and chlorite, sample SA 28.

Planche 1. Photo A : Tectonique extensive affectant les calcschistes de Santa Barbara. La foliation S_1 est déformé par les plans de cisaillements conjugués C_3 , échantillon SA2. Photo B : Calcschiste à albite-lawsonite avec les nodules d'albite incluant du quartz et de la lawsonite. Les calcites maclées traduisent une déformation de basse température, échantillon SA 2. Photo C : Eclogite de basse température à porphyroblastes de grenat et zoisite, échantillon S223. Photo D : Schiste bleu montrant des porphyroblastes de grenat à inclusions de zoisite et sphère entouré par une foliation schiste bleu définie par la glaucophane et la phengite. Le clinopyroxène, localement préservée dans les ombres de pression des grenats est partiellement déstabilisé en glaucophane, échantillon SA33. Photo E : Calcschiste à glaucophane montrant une zone de cisaillement C_3 affectant la foliation S_2 échantillon SA28. Photo F : Calcschiste à glaucophane. La tectonique extensive est caractérisée par un microboudinage perpendiculairement à l'allongement des glaucophanes. Les inter-boudins sont remplis par de la calcite et de la chlorite, échantillon SA28.

Table I. Representative microprobe mineral analyses used for thermobarometry estimates.**Tableau I.** Analyses microsondes représentatives des phases minérales utilisées pour les estimations thermobarométriques.

mineral	grt	grt	grt	grt	cpx	cpx	cpx	amph	amph	amph	pheng	pheng	parag	parag	zo	ep30	zo	zo	zo	zo	zo	czo	laws	albite	chlorite
sample	SA 2	SA 34 rim	SA 34 core	SA 28	S 223	SA 34	SA 33 rim	SA 28 gln	S 223 act	S 223 gln	SA 2 matrix	S 223 matrix	SA 28 inclusion	SA 34 matrix	SA 28	SA 28	S223 matrix	S223 inclusion	SA 33 matrix	SA 34 matrix	SA 34 matrix	SA 2	SA 2	S 223	
SiO ₂	36,36	37,42	37,04	37,30	56,24	56,08	55,07	56,60	55,33	58,80	49,49	50,92	46,06	46,58	37,31	36,92	39,83	38,57	38,02	38,83	38,38	38,16	68,89	27,21	
TiO ₂	0,13	0,02	0,17	0,04	0,07	0,01	0,03	0,01	0,00	0,00	0,07	0,19	0,05	0,00	0,07	0,08	0,00	0,16	0,06	0,15	0,06	0,26	0,00	0,03	
Al ₂ O ₃	20,87	21,12	21,21	21,03	11,10	11,67	9,69	10,15	3,44	11,96	27,43	27,56	37,73	40,01	24,74	23,62	32,71	28,90	28,12	30,01	32,33	21,47	19,63	20,41	
FeO _(tot)	12,53	28,75	27,20	23,55	3,37	5,51	5,22	12,48	9,14	8,36	2,32	2,50	0,68	0,33	11,58	12,71	1,25	6,68	6,37	3,98	0,76	0,17	0,03	23,55	
MnO	19,86	0,46	2,41	6,42	0,04	0,01	0,07	0,18	0,04	0,03	0,08	0,03	0,00	0,00	0,25	0,51	0,00	0,27	0,07	0,47	0,06	0,01	0,03	0,31	
MgO	0,50	1,98	2,34	1,09	8,65	7,09	8,68	10,02	17,51	11,27	3,52	3,61	0,30	0,03	0,01	0,02	0,03	0,10	0,02	0,05	0,00	0,00	0,00	16,94	
CaO	8,68	10,35	9,08	10,74	13,75	11,90	14,22	0,57	11,21	0,57	0,09	0,03	0,11	0,08	23,28	23,09	24,68	23,83	23,89	23,02	24,54	17,70	0,07	0,03	
Na ₂ O	0,05	0,02	0,05	0,04	6,88	7,68	6,59	7,03	1,49	7,45	0,31	0,43	6,76	7,80	0,01	0,01	0,00	0,01	0,01	0,02	0,00	0,01	11,68	0,03	
K ₂ O	0,01	0,00	0,44	0,02	0,00	0,00	0,00	0,00	0,05	0,03	9,41	10,46	0,95	0,22	0,12	0,00	0,00	0,00	0,02	0,24	0,25	0,00	0,08	0,05	
Cr ₂ O ₃	0,04	0,03	0,06	0,02	0,00	0,05	0,02	0,00	0,00	0,00	0,06	0,06	0,06	0,04	0,02	0,02	0,00	0,00	0,06	0,13	0,08	0,03	0,00	0,03	
Total	99,01	100,15	99,99	100,24	100,09	100,00	99,59	97,04	98,21	98,47	92,78	95,79	92,70	95,09	99,25	98,84	98,50	98,52	98,55	98,83	98,41	87,82	100,42	88,59	
Si	2,95	2,97	2,94	2,97	1,99	2,00	1,99	7,86	7,73	7,91	3,37	3,36	3,04	2,98	2,97	2,97	3,00	2,96	2,99	3,01	2,97	2,02	3,00	2,80	
Ti	0,01	0,00	0,01	0,00	0,00	0,00	0,00	0,00	0,00	0,00	0,00	0,01	0,00	0,00	0,00	0,00	0,00	0,01	0,00	0,01	0,00	0,01	0,00	0,00	
Al ^{IV}	0,05	0,03	0,06	0,03	0,01	0,00	0,01																		
Al ^{VI}	1,95	1,94	1,92	1,94	0,46	0,49	0,40																		
Al								1,66	0,57	1,90	2,20	2,14	2,93	3,01	2,32	2,24	2,90	2,61	2,61	2,75	2,95	1,96	1,00	2,48	
Fe ²⁺	0,76	1,82	1,64	1,48				0,82	0,85	0,76	0,13	0,12	0,38	0,02	0,00	0,00	0,00	0,00	0,00	0,00	0,00	0,01	0,00	2,03	
Fe ³⁺	0,09	0,09	0,17	0,09				0,56	0,20	0,16					0,69	0,77	0,08	0,43	0,38	0,23	0,04	0,00	0,00	0,00	
Fe _{tot}					0,10	0,16	0,16																		
Mn	1,37	0,03	0,16	0,43	0,00	0,00	0,00	0,02	0,01	0,00	0,00	0,00	0,00	0,00	0,02	0,03	0,00	0,02	0,00	0,03	0,00	0,00	0,00	0,03	
Mg	0,06	0,23	0,28	0,13	0,46	0,38	0,47	2,07	3,65	2,26	0,36	0,35	0,30	0,00	0,00	0,00	0,00	0,01	0,00	0,01	0,00	0,00	0,00	2,60	
Ca	0,76	0,88	0,77	0,92	0,52	0,45	0,55	0,09	1,68	0,08	0,01	0,00	0,01	0,01	1,99	1,99	1,99	1,96	2,01	1,91	2,04	1,00	0,00	0,00	
Na	0,01	0,00	0,01	0,01	0,47	0,53	0,46	1,89	0,40	1,95	0,04	0,05	0,86	0,97	0,00	0,00	0,00	0,00	0,00	0,00	0,00	0,00	0,00	0,99	
K	0,00	0,00	0,04	0,00	0,00	0,00	0,00	0,00	0,01	0,01	0,82	0,88	0,00	0,02	0,01	0,00	0,00	0,00	0,00	0,02	0,02	0,00	0,00	0,01	
Cr	0,00	0,00	0,00	0,00	0,00	0,00	0,00	0,00	0,00	0,00	0,00	0,00	0,00	0,00	0,00	0,00	0,00	0,00	0,00	0,01	0,00	0,00	0,00	0,00	
Alm	26	61	57	50	Jad	45	49	39																Ab	
Gross	25	29	27	31	Acm	2	4	6																An	
Pyr	2	8	10	4	Aug	53	47	55																An	
Spess	46	1	6	15																				0,4	

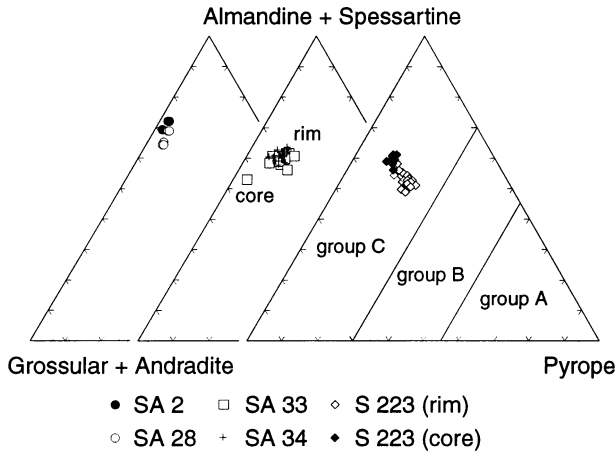


Figure 6. Garnet composition. Fields A, B and C are from [26].
Figure 6. Composition des grenats, champs A, B, C définis par [26].

Zoisites are common in the HP unit, and absent in the LP unit which is characterized by the presence of stable lawsonite. The metabasalts of the HP unit show a great abundance and variety of epidotes corresponding to various metamorphic stages. In the eclogite S223, one can distinguish three generations of epidotes:

- zoisite included in garnets with a Fe_2O_3 content varying from 6.56 to 8.21 wt.%,
- abundant zoisite in the matrix, with FeO content varying from 1 wt.% to 1.8 wt.%,
- Fe-epidote ($Fe_2O_3 = 9.2$ wt.%) in fractured garnet is associated with Fe-chlorite.

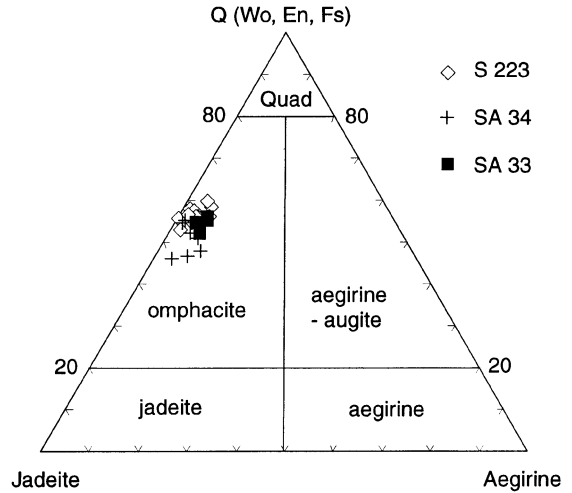


Figure 8. Pyroxene composition of Punta Balandra metabasalts in the quad-jadeite-aegirine system [28].

Figure 8. Composition des pyroxènes des metabasalts de l'unité de Punta Balandra dans le diagramme de Morimoto [28].

Eclogite SA34 and blueschist SA33 show inclusions of Fe-rich zoisite ($Fe_2O_3 = 8.5$ wt.%) in the garnet core. The eclogite SA34 is also characterized by the presence of zoisite and clinozoisite closely associated with paragonite. This assemblage is typical of the destabilisation of lawsonite. The Fe_2O_3 content of the zoisites varies from 3.2 to 4 wt.% and it is approximately 0.8 wt.% for the clinozoisites. SA33 is marked by the crystallization of rare zoisites ($Fe_2O_3 = 6.4$ to 7 wt.%), within the matrix. Zoisites, clinozoisites and epi-

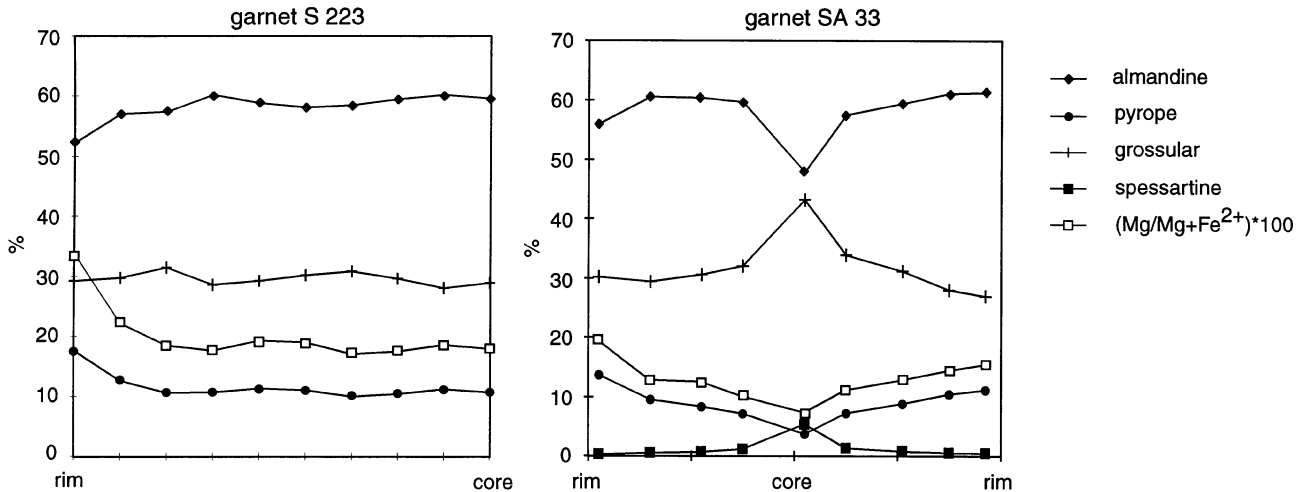


Figure 7. Chemical profiles of garnet in two Punta Balandra metabasalts (S223 and SA33).

Figure 7. Profiles de zonation chimique dans les metabasalts S223 et SA33 de l'unité de Punta Balandra.

dots are also present in the micaschist SA28. Clinozoisite appears only as inclusions in glaucophane. In the matrix, a zoisite of lower size is well crystallized and directly associated to the foliation S_2 . Epidotes grow over previous parageneses. All these epidotes show a significant substitution of Al_2O_3 by Fe_2O_3 . The Fe_2O_3 contents varies from 7.8 wt.% in the clinozoisites to 12.7 wt.% in late epidotes. These compositional variations are consistent with those of glaucophanes which are also rich in iron, reflecting the whole-rock composition.

Plagioclase corresponds to a retrograde phase under greenschist facies conditions. It appears in the fractures of garnets associated with chlorite and calcite or as large crystals within the matrix (SA33 and SA34). The composition is also close to the pure albite endmember (Ab_{98}).

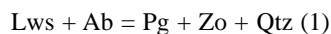
Chlorite is a common mineral of the HP unit, where it primarily seems to be a product of the destabilisation of garnet, often associated with albite and corresponds to greenschist facies conditions. Their FeO content varies from 15.6 to 18.3 wt.% in the eclogite S223 and from 22.4 to 24 wt.% in SA13. Fe-rich chlorite inclusions ($FeO > 31$ wt.%), appear in the S223 garnet.

5. Thermobarometric estimates

In order to validate the thermobarometric estimates, three complementary methods were used and compared according to the approach discussed by Guillot et al. [29]. It is based on: 1) a petrogenetic grid built on the experimental stability field of mineral phases, 2) conventional Fe-Mg exchange thermometry, pressure estimate is made difficult by the absence of primary plagioclase which only makes it possible to consider minimal pressures according to the jadeite content in omphacite, 3) the Thermocalc program, based on the thermodynamic data of Powell and Holland [30–32]. This program makes it possible to calculate all the reactions between the pure poles of the phases belonging to a same paragenesis and then to evaluate the P–T conditions of the analyzed mineralogical assemblage; when the fit is inferior or close to 1.0, the P–T estimates are valid. All the data are compiled in *figure 9*. Uncertainties are given at 2σ .

5.1. Unit of Santa Barbara

The presence of the stable assemblage albite + lawsonite implies that sample SA2 is located on the low temperature side of the reaction [33]:



i.e. at a temperatures lower than 400 °C. The use of the garnet-phengite geothermometer [34] on three mineral pairs gives a temperature of 330 °C, compatible with the stability of albite + lawsonite. The Thermocalc program, applied to

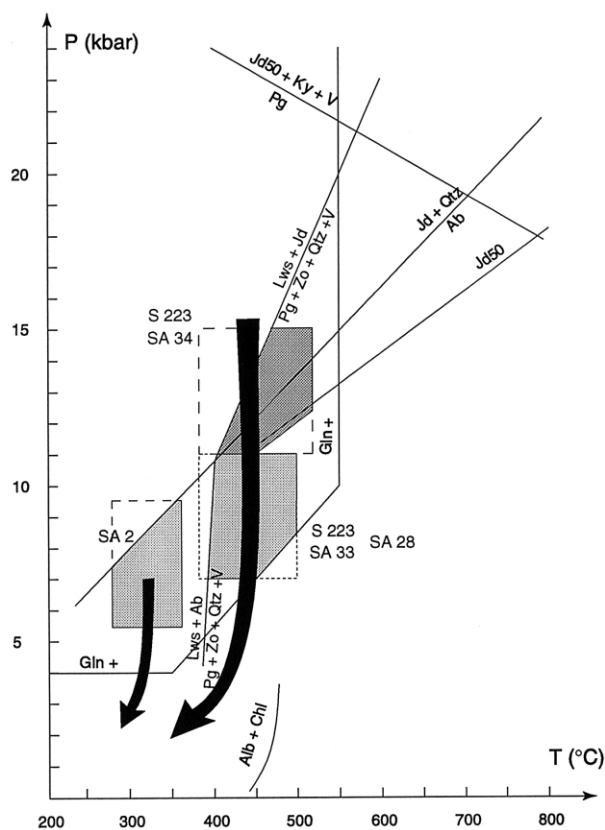


Figure 9. P-T path of Santa Barbara (SA2) and Punta Balandra (SA28-33-34, S223) samples.

Figure 9. Trajet P-T des échantillons de Santa Barbara (SA2) et de Punta Balandra (SA28-33-34, S223).

the paragenesis Mn-garnet, albite, lawsonite, phengite, calcite and quartz indicates a temperature of 310 ± 40 °C (fit = 1.5).

The absence of jadeite, associated with the presence of albite, suggests a maximum pressure of 8.5 kbar for 330 °C. The pressure estimated by Thermocalc on the paragenesis Mn-garnet, albite, lawsonite, phengite, calcite and quartz is of 7.5 ± 2 kbar (fit = 1.3). The combination of the three methods supports the pressure–temperature conditions in the unit of Santa Barbara at 320 ± 40 °C and 7.5 ± 2 kbar.

5.2. Unit of Punta Balandra (HP)

5.2.1. Eclogitic stage

The eclogitic stage, in the sample S223, occurs at a minimal temperature of 450 °C at 14 kbar according to the zoning of garnet, and by the stability of zoisite [33]. The temperatures obtained according to the geothermometry based on the Fe-Mg exchange are compatible with previous data.

The temperature obtained by using the calibrations of Ellis and Green, 1979 [34] and Powell, 1985 [35] is of 450 ± 80 °C. The garnet-phengite thermometer [36] applied to the phengites included in garnets gives a temperature of 480 ± 40 °C. The Thermocalc program was used on the garnet, omphacite, zoisite, paragonite, rutile and quartz assemblage. This method leads to a temperature of 460 ± 80 °C (fit = 0.6). The presence of omphacite with a maximum $X_{\text{Jd}} = 0.45$, indicates a minimal pressure of 11.5 kbar for 460 °C in presence of quartz. The use of Thermocalc on the same eclogitic assemblage allows a more precise estimate of the pressure at 14 ± 2 kbar (fit = 0.5).

The P–T conditions for the eclogitic assemblage of the sample S223 are then of 460 ± 70 °C and 14 ± 2 kbar (figure 9).

Eclogite SA34 is characterized by the presence in the matrix of zoisite associated with paragonite suggesting a minimal temperature of about 430 °C at 13 kbar. The application of the thermometer of Ellis and Green, 1979 [34] on 6 garnet-clinopyroxene pairs provides a temperature estimate of 410 ± 140 °C. The thermometer [36] on 3 garnet-phengite pairs gives a temperature of 450 ± 20 °C. The Thermocalc program allows a temperature of 440 ± 50 °C (fit = 0.7) on the eclogitic paragenesis of garnet, omphacite, zoisite, paragonite, rutile and quartz. The presence of paragonite coupled with the absence of kyanite within the matrix implies a pressure lower than 23 kbar at 440 °C. The jadeite content of pyroxene ($X_{\text{Jd}} = 49\%$) imposes a minimal pressure of approximately 11 kbar. The use of the Thermocalc program on the same eclogitic assemblage leads to a pressure of 13 ± 1 kbar (fit = 0.7).

By combining the three methods, one can thus consider the physical conditions of the eclogitic metamorphism in the sample SA34 at 430 ± 80 °C and 13 ± 1 kbar (figure 9).

5.2.2. Blueschist stage

In the sample S223, the stability of glaucophane during decompression implies a temperature lower than 480 °C at 8 kbar [37]. Moreover abundance of zoisite suggests that the temperature was higher than 400 °C, according to the reaction (2). A temperature of 470 ± 50 °C, compatible with the mineralogical constraints, was calculated with the garnet-phengite thermometer of Krogh and Raheim [36]. The use of the Thermocalc program on the blueschist assemblage in the matrix (rim of garnet, glaucophane, zoisite, phengite, titanite and quartz) indicates a temperature of 470 ± 100 °C (fit = 1.8). Because of the absence of albite and omphacite in this paragenesis, the pressure can not be estimated by conventional barometry. On the other hand, the application of the Thermocalc program indicates a pressure of 8 ± 2 kbar (fit = 0.6). By combining the three methods, the P–T conditions estimated for the blueschist facies paragenesis are 470 ± 80 °C and 8 ± 2 kbar (figure 9).

The metabasalt SA33 is characterized by the presence of glaucophane, phengite and rare zoisites in the matrix. The same estimated conditions for the sample S223 may be envisaged, namely a temperature ranging between 400 and 520 °C for a pressure of 9 kbar. The garnet-phengite thermometer [36] indicates a temperature of 400 ± 40 °C. Temperatures obtained from Thermocalc on the SA33 paragenesis (garnet-rim, glaucophane, phengite, zoisite and titanite) are slightly higher than the data obtained by conventional thermometry, at 450 ± 80 °C (fit = 1.2). The barometric estimates may be carried out only with Thermocalc program on the same assemblage. The result obtained on the blueschist paragenesis is 9 ± 2 kbar (fit = 1.2). The P–T conditions of the blueschist stage can be summed up for the sample SA 33 at 430 ± 60 °C and 9 ± 2 kbar (figure 9).

The blueschist assemblage for the micaschist SA28 consists of garnet, glaucophane, zoisite, phengite, clinozoisite and paragonite. Glaucophane-zoisite association constrains the temperature between 400 and 550 °C for 10 kbar, according to the stability field of glaucophane [37] and the reaction (2). The thermometer of Krogh and Raheim [36] applied to the phengites of the matrix in contact with garnets gives a temperature of 440 ± 40 °C. The Thermocalc application on the garnet-rim, glaucophane, phengite and zoisite paragenesis in the matrix leads to a temperature of 390 ± 80 °C (fit = 1.3). The pressure is only estimated by Thermocalc on the same paragenesis (10 ± 2 kbar; fit = 1.3). Average P–T conditions on SA28 are estimated at 420 ± 60 °C and 10 ± 2 kbar (figure 9).

5.2.3. Greenschist stage

The late evolution under greenschist facies conditions may not have been precisely evaluated. The late occurrence of chlorite in all samples belonging to the Punta Balandra unit implies a temperature lower than 500 °C [27]. Eclogite SA34 and associated SA33 metabasalt contain a typical greenschists assemblage (albite + chlorite + titanite + calcite) in the fractures of garnet and in the matrix. This mineral association is limited to a maximum temperature of 400 °C [27]. The absence of pumpellyite, at the equilibrium with chlorite (or actinolite), imposes a minimal temperature of about 300 °C [27].

6. Discussion and conclusions

The new petrological and thermobarometric data presented in this work confirm the existence, in the peninsula of Samaná, of two tectonic units characterized by a different metamorphic imprint [15]. We propose a precise quantification of the intensive parameters of the metamorphism in the two units. The maximum P–T conditions of the Santa Barbara unit (LP) are of 320 ± 40 °C and 7.5 ± 2 kbar. The coherent metamorphic evolution (figure 9) of metabasalts (S223 and SA34 / SA33) allows the precise definition of the

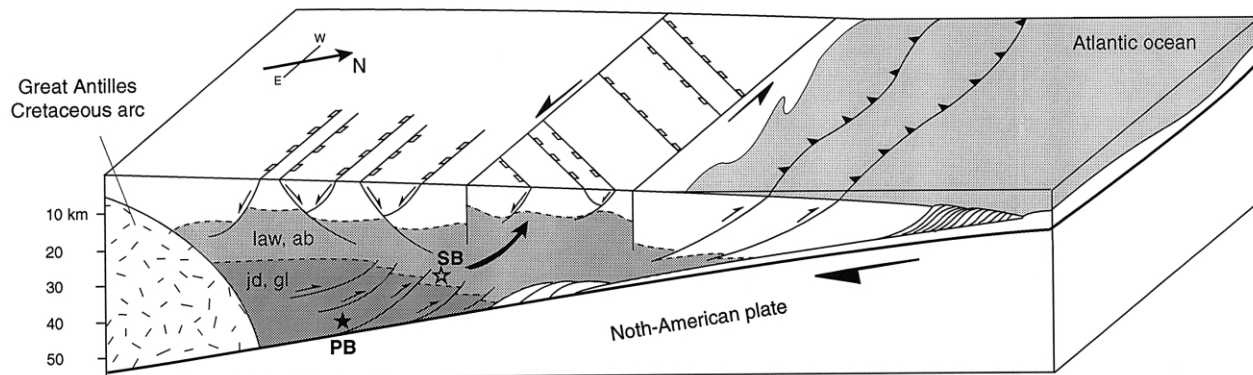


Figure 10. Model of tectonic uplift and exhumation of HP-LT units in an accretionary wedge, modified after [4, 10], and applied to the Samaná Peninsula.

Figure 10. Modèle d'exhumation des roches de HP-BT au sein d'un prisme d'accrétion, modifié d'après [4, 10], et appliqué à la Péninsule de Samaná.

P–T evolution of the Punta Balandra unit. The well-preserved eclogitic parageneses show systematically petrographic and thermodynamic evidence of retrogression under blueschist, and the greenschist facies conditions. The maximum conditions of the metamorphism were estimated at about 13 ± 2 kbar for a temperature of 450 ± 70 °C. The blueschist facies decompression was strictly isothermal with a temperature of about 440 ± 60 °C for a pressure of 9 ± 2 kbar (figure 9). Thus, the petrological data show that these two units do not correspond to a continuous metamorphic zonation but to two different metamorphic evolutions, recording different depths of subduction. According to our estimates, the pressure difference between them is of about 6–7 kbar. Moreover, the zone between the two units described by Joyce [13] as an intermediate metamorphic zone is characterized by relicts of eclogitic minerals in the D_2 foliation, and consequently the top-to-NNE sense of shear developed during D_2 is interpretable in terms of thrusting of the HP unit onto the LP metamorphic unit of Santa Barbara, under blueschist facies conditions (figures 3 and 4). Finally, the end of the exhumation of the two units is controlled by the development of NW–SW conjugate normal fault under greenschist facies conditions.

Association of lenses of metabasalts, carbonates, micaschists in very thin lithotectonic units (< 1 km) separated by thrust fault and characterized by contrasting P–T is typical of an accretionary wedge such as the Californian Franciscan complex [4, 38]. This suggests that the peninsula of Samaná is a fragment of an accretionary wedge developed during the Upper Cretaceous subduction of the oceanic part of the North American plate [23, 24]. Indeed, the dynamic evolution of an accretionary wedge is characterized by a partitioning of the deformation in space and time, since the bottom of the prism is affected by thrust tectonics with a vergence opposite to the dip of the subduction plane, while the

top of the prism is subjected to superficial extension, and strike-slip faulting in its frontal part [4]. The HP thrusting of the Punta Balandra unit over the Santa Barbara unit is therefore compatible with the dynamics of the base of an accretionary wedge, and partly explains the exhumation of HP rocks (figure 10). This suggests that the first part of the exhumation of the Punta Balandra eclogite under blueschist facies conditions occurred by thrusting within an accretionary wedge. In this global context, the unknown contact between the Santa Barbara unit and the Rincon Marbles would also be interpreted as a thrusting structure (figure 4).

However, the occurrence of a sinistral strike-slip component during D_2 and D_3 suggests that the exhumation of the HP-LT rocks occurred in an oblique convergent context that should be explained at the plate tectonic scale. In fact, the North Caribbean margin was characterized, during the Middle Eocene, by a major change in the kinematic direction that corresponds to the end of the subduction of the North Caribbean plate and its oblique collision with the North American shelf. This led to the setting of a sinistral strike-slip tectonics of east–west direction [12, 39]. The direction of D_2 thrusting towards the NNE is compatible with the supposed direction of convergence of the Caribbean and North American plates before the Eocene collision [39], i.e. an active subduction context towards the SSW. However, the non-orthogonality between the D_2 fold of $N140^\circ$ direction and the $N20^\circ$ stretching direction may correspond to the onset of the sinistral strike-slip tectonics while the oceanic subduction was still active.

The ultimate exhumation of these units is driven by the development of conjugate extension of NW–SE direction which is not directly compatible with the growth of an accretionary wedge with a NE–SW direction of convergence. Indeed, the development of a late extension under the green-

schist facies conditions to the back of an accretionary wedge is a current feature [4], but the direction of extension is usually parallel to the direction of convergence. In the case of the peninsula of Samaná, the direction of extension is perpendicular with the earlier direction of convergence, implying a major change in the direction of strain and thus a major change at the boundary plates. Mann and Gordon [10] suggest, on different examples in the world and more particularly for the case here concerned, that large active strike-slip faulting may play a significant role in the end of exhumation of HP rocks. However, these authors propose that in the case of the peninsula of Samaná, the final context of exhumation of the HP rock is transpressive. However, the development of sinistral E–W wrenching in the central and western part of Hispaniola and the opening of the Caiman pull-apart oceanic at the end of Eocene may be better explained by a transtensive tectonic regime, with an ENE–WSW direction of convergence (*figure 1*). Thus, we interpret the development of the conjugate extension in the peninsula of Samaná as a consequence of a transtensive tectonic regime, affecting the higher part of the accretionary wedge (*figure 10*). The development of this transtensive regime may be related to a kinematic change between the Caribbean plate and the North American plate from a NNE–SSW to ENE–WSW direction of convergence during the Eocene, leading to the eastward migration of the active subduction under the Lesser Antilles [12].

Acknowledgements. This work was financed by the project INSU-CNRS “Intérieur de la Terre”. We are very grateful to Michele Veschambre for the microprobe analyses. We greatly appreciate reviews by G. V. Dal Piaz and R.G. Coleman.

References

- [1] Allemand P., Lardeaux J.M., Strain partitioning and metamorphism in a deformable orogenic wedge; Application to the Alpine belt, *Tectonophysics* 280 (1997) 157–169.
- [2] Chemenda A.I., Mattauer M., Malavieille, Bokun A.N., A mechanism for syncollisional rock exhumation and associated normal faulting, *Earth Planet. Sci. Lett.* 132 (1995) 225–232.
- [3] Duchêne S., Lardeaux J.M., Albarède F., Exhumation of eclogites: insights from depth-time path analysis, *Tectonophysics* 280 (1997) 125–140.
- [4] Platt J.P., Dynamic of orogenic wedges and the uplift of high-pressure metamorphic rocks, *Bull. Geol. Soc. Am.* 97 (1986) 1037–1053.
- [5] Cloos M., Thermal evolution of convergent plate margins: thermal modeling and re-evaluation of isotopic Ar ages for blueschists in the Franciscan complex of California, *Tectonics* 4 (1985) 421–433.
- [6] Blake M.C., Brothers R.N., Lanphere M.A., Radiometric ages of blueschists in New Caledonia, in: *International symposium on geodynamics in south-west Pacific*, Ed. Technip, Nouméa, 1976, pp. 279–281.
- [7] Maekawa H., Chozui M., Ischii T., Friyer P., Pearce A., Blueschist metamorphism in an active subduction zone, *Nature* 364 (1993) 520–523.
- [8] Ernst W.G., Tectonic history of subduction zones inferred from retrograde blueschist P–T paths, *Geology* 16 (1988) 1081–1084.
- [9] Spalla M.I., Lardeaux J.M., Dal Piaz G.V., Gosso G., Messiga B., Tectonic significance of alpine eclogites, *J. Geodyn.* 21 (1996) 257–285.
- [10] Mann P., Gordon M.K., Tectonic uplift and exhumation of blueschists belts along transpressional strike-slip fault zones, in: Bebout G.E., Scholl D.W., Kirby S.H., Platt J.P. (Eds.), *Subduction top to Bottom*, Geophy. Mono. Series, 96, 1996, pp. 143–154.
- [11] Sigoyer J. de, Mécanismes d’exhumation des roches de haute pression haute température en contexte de convergence continentale (Tso Moriri, NW Himalaya), thèse université de Lyon, 1998, 236 p.
- [12] Pindell J.L., Barrett S.F., Geological evolution of the Caribbean region: A plate-tectonic perspective, in: Dengo G., Case J.E. (Eds.), *The Caribbean region: Boulder, Colorado*, Geol. Soc. Am., *The Geology of North America*, 1990, pp. 405–432.
- [13] Joyce J., Blueschist metamorphism and deformation on the Samaná Peninsula: A record of subduction and collision in the Greater Antilles, in: Mann P., Draper G., Lewis J.F. (Eds.), *Geologic and tectonic studies of the North American-Caribbean plate boundary in Hispaniola*, Geol. Soc. Am. Sp. Paper, 262, 1991, pp. 47–75.
- [14] Mercier de Lépinay B., L’évolution géologique de la bordure nord-Caraïbe : l’exemple de la transversale de l’île d’Hispaniola (Grandes Antilles), thèse de doctorat d’État, université Pierre-et-Marie Curie, 1987, 374 p.
- [15] Nagle F., Blueschist, eclogite, paired metamorphic belts, and the early tectonic history of Hispaniola, *Bull. Geol. Soc. Am.* 85 (1974) 1461–1466.
- [16] Fox P.J., Henzen B.C., Geology of the Caribbean Crust, in: Nairn A.E.M., Stehli F.G. (Eds.), *Ocean and Basin Margins*, 3: *The Caribbean and Gulf of Mexico*, Plenum Press, New-York, 1975, pp. 421–466.
- [17] Perfit M.R., Heezen B.C., Rawson M., Donnelly T.W., Metamorphic rocks from the Puerto Rico trench: their origin and tectonic significance, *Marine Geology* 34 (1980) 125–156.
- [18] Boiteau A., Michard A., Saliot P., Métamorphisme de haute pression dans le complexe ophiolitique de Purial (Oriente, Cuba), *C. R. Acad. Sci.*, Paris 274 (1972) 2137–2140.
- [19] Millan G., Somin M.L., Litología, estratigrafía, tectónica, y metamorfismo del macizo de Escambray, Editorial Academia, La Havane, Cuba 452, 1981, 104 p.
- [20] Coleman R.G., Somin M., Millan G., Dobrestov N., Tectonic significance of eclogites in Cuba, *EOS* 79 (1998) F989 p.
- [21] Weaver J.D., Panella G., Llinas-Castellan, Preliminary sketch of the tectonic history of the Samaná Peninsula, Dominican Republic, presented at “3rd Congreso Latino-Americano de Geología”, Mexico, 1976.
- [22] Calais E., Mercier de Lépinay B., Strike-slip tectonic processes in the Northwestern Caribbean between Cuba and Hispaniola (Windward Passage), *Marine Geophys. Res.* 17 (1992) 63–95.
- [23] Joyce J., Aronson J., K/Ar ages for blueschists metamorphism on the Samaná Peninsula, Dominican Republic, 10th Caribbean Geol. Conf., Abstracts, Cartagena, Colombia, 1983, 44.
- [24] Perfit M.R., McCulloch M.T., Nd- and Sr-isotope geochemistry of eclogites and blueschists from the Hispaniola-Puerto Rico subduction zone, *Terra Cognita* 2 (1982) 325 p.
- [25] Liou J.G., Maruyama S., Parageneses and compositions of amphiboles from Franciscan jadeite-glaucophane type facies series

metabasalts at Cazadero, California, *J. Metam. Geol.* 5 (1987) 371–395.

[26] Coleman R.G., Lee D.E., Betty L.B., Brannock W.W., Eclogites and eclogites: their differences and similarities, *Bull. Geol. Soc. Am.* 76 (1965) 483–508.

[27] Spear F.S., *Metamorphic Phase Equilibria and Pressure-Temperature-Time Paths*, Mineral. Soc. Am., 1993, 799 p.

[28] Morimoto N., Nomenclature of Pyroxenes, *Bull. Mineral.* 111 (1988) 535–550.

[29] Guillot S., de Sigoyer J., Lardeaux J.M., Mascle G., Eclogitic metasediments from the Tso Moriri area (Ladakh, Himalaya): evidence for continental subduction during India-Asia convergence, *Contrib. Mineral. Petrol.* 128 (1997) 197–212.

[30] Powell R., Holland T.J.B., An internally consistent thermodynamic dataset with uncertainties and correlations: 1. Methods and worked examples, *J. Metam. Geol.* 3 (1985) 327–342.

[31] Powell R., Holland T.J.B., An internally consistent thermodynamic dataset with uncertainties and correlations: 3. Applications to geobarometry, worked examples and a computer program, *J. Metam. Geol.* 6 (1990) 173–204.

[32] Holland T.J.B., Powell R., An internally consistent thermodynamic dataset for phases of petrological interest, *J. Metam. Geol.* 16 (1998) 309–343.

[33] Heinrich H., Althaus E., Experimental determination of the 4 lawsonite + 1 albite = 1 paragonite + 2 zoisite + 2 quartz + 6H₂O and 4 lawsonite + 1 jadeite = 1 paragonite + 2 zoisite + 2 quartz + 6H₂O, *Neues Jahrb Mineral Monatsh* 11 (1988) 516–528.

[34] Ellis D.J., Green D.H., An experimental study of the effect of Ca upon garnet-clinopyroxene Fe-Mg exchange equilibria, *Contrib. Mineral. Petrol.* 71 (1979) 13–22.

[35] Powell R., Regression diagnostic and robust regression in geothermometer/geobarometer calibration: the garnet-clinopyroxene geothermometer revisited, *J. Metamorphic Geol.* 3 (1985) 231–243.

[36] Krogh E.J., Raheim A., Temperature and pressure dependence of Fe-Mg partitioning between garnet and phengite with particular references to eclogites, *Contrib. Mineral. Petrol.* 66 (1975) 75–80.

[37] Maresh W.V., Experimental study on glaucophane, an analysis on present knowledge, *Tectonophysics* 43 (1977) 109–125.

[38] Cloos M., Blueschists in the Franciscan Complex of California: Petrotectonic constraints on uplift mechanisms, *Geol. Soc. Am. Mem.* 164 (1986) 77–93.

[39] Mann P., Draper G., Lewis J.F., An overview of the geologic and tectonic development of Hispaniola, *Geol. Soc. Am. Spec. Paper* 262 (1991) 1–27.